Polymer Degradation and Stability 169 (2019) 108981

Contents lists available at ScienceDirect

Polymer Degradation and Stability

journal homepage: www.elsevier.com/locate/polydegstab

Synthesis of a novel phosphorus-nitrogen flame retardant and its application in epoxy resin

Zong-Min Zhu [a], Luo-Xin Wang [a], Xue-Bao Lin [b, *], Liang-Ping Dong [c]

[a] College of Materials Science and Engineering, State Key Laboratory of New Textile Materials and Advanced Processing Technologies, Wuhan Textile University, 430200, Wuhan, Hubei, PR China
[b] Zhuzhou Times New Material Technology Co.,Ltd, 412007, Zhuzhou, Hunan, PR China
[c] Institute of Electronic Engineering, China Academy of Engineering Physics, 621000, Mianyang, Sichuan, PR China

ARTICLE INFO

Article history:
Received 29 July 2019
Received in revised form
17 September 2019
Accepted 22 September 2019
Available online 23 September 2019

Keywords:
Epoxy resin
Flame retardancy
Smoke suppression
Thermal behavior
Mechanism

ABSTRACT

A novel phosphorus-nitrogen flame retardant named as melamine phenyl phosphate (MAPPO) was synthesized successfully via the neutralization reaction between phenylphosphonic acid (PPOA) and melamine (MA). The chemical structure of MAPPO was characterized by Fourier transform infrared spectra (FT-IR), nuclear magnetic resonance (NMR) and element analysis (EA). MAPPO was introduced into epoxy resin by blending to improve the flame retardancy. Flame retardancy and combustion behavior of EP/MAPPO were investigated by limiting oxygen index (LOI) test, vertical burning (UL-94) test and cone calorimeter test. UL-94 and LOI tests results showed EP containing 18 wt% MAPPO passed the UL-94 V-0 rating and got a high LOI value of 33%. In the cone calorimeter test, compared with that of EP, the values of peak of heat release rate (HRR), total heat release (THR), peak of smoke production rate (PSPR) and total smoke production (TSP) of modified EP were reduced by 58.7%, 40%, 49% and 61.6%, respectively. By analyzing the volatile pyrolysis products of MAPPO, it was known that MAPPO mainly produced CO_2, NH_3, H_2O and other nitrogen-containing compounds, which diluted the concentration of fuel gases and oxygen during combustion. Meanwhile, the char residue of EP/MAPPO system after combustion was also analyzed by scanning electron microscope (SEM), FT-IR and Raman tests, and the results showed MAPPO was able to promote the crosslinking of EP leading to the formation of compact char layer containing P—O—C, P═O and C═C, etc. In a word, the enhancement in flame retardancy was attributed to both dilution effect of non-combustible gases and barrier effect of compact char.

1. Introduction

As one of the most common used thermoset polymers, epoxy resins are widely used in the fields of adhesives, coatings, aerospace & aviation, composites and electronic circuit board because of its good adhesive property, excellent dimensional stability, high mechanical strength, outstanding chemical resistance and excellent dielectric performance [1–6]. However, the inherent flammability and lots of smoke production defects of epoxy resin (EP) which seriously restricts its application in many fields to a certain extent.

For the current industrial products, adding a small amount of halogen-containing flame retardants is a normal way to improve the flame retardancy of EP, but halogen-containing EP composites will produce some toxic or smoke during combustion, which leads to the harms to the environment and human safety as well [7,8]. Hence, it is necessary to develop the efficient and environmentally friendly flame retardants to replace halogen-containing one for solving the above problems.

To date, a variety of halogen-free flame retardants have been developed to improve the fire retardancy of EP, including inorganic hydroxides [9–11], organic phosphorus-containing flame retardants [12–16] and intumescent fire retardants (IFR) [17–19]. Due to low flame-retardant efficiency, high loading of inorganic hydroxides are always required, which compromise to the mechanical properties. Although organic phosphorus-containing flame retardants can endow satisfied flame retardancy of EP, their smoke production has not been well inhibited. For example, Xu et al. [20] prepared a novel DOPO-based curing agent (IHODOPO) derived from DOPO and imidazole for EP, and fire tests results presented that EP containing 15 wt% IHODOPO can pass the UL-94

* Corresponding author.
E-mail address: tian09jing24@gmail.com (X.-B. Lin).

https://doi.org/10.1016/j.polymdegradstab.2019.108981
0141-3910/

V-0 rating and achieved a LOI value of 37%, while the smoke production was increased compared with that of neat EP. Intumescent flame retardant (IFR) is considered to be a promising method for imparting EP with expected flame retardancy, more importantly, which can effectively achieve smoke suppression effect due to its condensed phase activity [21–24]. Basically, IFR consists of an acid source, a charring agent and a gas source. Once the material containing IFR is ignited, the intumescent char structure can be developed through the dehydration, charring and foaming process, which restrains the heat and oxygen transfer, thereby improving the flame retardancy and smoke suppression. For non-charring resins, IFR/resin system can be constructed with above three components, while only the acid source and gas source are required to prepare IFR/EP system because of the good charring ability of EP. In most cases, some phosphorous-nitrogen containing flame retardants, such as melamine cyanurate (MCA), melamine phosphate (MP), melamine polyphosphate (MPP) and ammonium polyphosphate (APP) can provide the acid source and gas source for IFR/EP system [25–28]. By the comparison with the previous three flame retardants, APP possesses a relatively high flame-retardant efficiency, but adding 20 wt% APP still can not make EP pass V-0 rating [29]. In addition, the poor compatibility between inorganic IFRs (MCA, MP, MPP and APP) with EP matrix also resulted in the decrease of flame retardancy.

To address some of above problems, a novel organic melamine phosphonate intumescent flame retardant was synthesized by the neutralization reaction between phenylphosphonic acid (PPOA) and melamine (MA) for EP. A series of flame-retardant EP was obtained by introducing different amount of MAPPO. Thermal stabilities and charring abilities of MAPPO and EP/MAPPO samples were investigated by TG. Fire retardancy and combustion behavior of EP and EP/MAPPO samples were investigated by LOI, UL-94 and cone calorimeter tests. Besides, the flame-retardant mechanism of MAPPO was also studied by TG-IR, SEM, FT-IR and Raman tests.

2. Experimental

2.1. Materials

Diglycidyl ether of bisphenol A (DGEBA, E−44) was obtained by Nantong Xingchen Synthetic Material Co., Ltd. (Nantong, China). 4, 4′- Diamino diphenylmethane (DDM) and melamine (MA) were purchased from Sinopharm Chemical Reagent Co., Ltd. (Shanghai, China). Phenylphosphonic acid (PPOA) was purchased from Aladdin Chemistry Co., Ltd. (China). Distilled water was obtained by our Lab.

2.2. Synthesis of flame retardant melamine phenyl phosphate (MAPPO)

Route for synthesis of MAPPO was shown in Scheme 1. Firstly, phenylphosphonic acid (7.9 g, 0.05 mol) and 200 mL deionized water were added into a 500 mL three-neck flask equipped with a mechanical stirrer and reflux condenser. Then the mixture was heated to 100 °C with continuous stirring. After that, melamine (12.6 g, 0.1 mol) was added to flask by twice in 20 min. After finishing, the solution was kept stirring for 5 h. Finally, the reaction solution was cooled slowly to room temperature. The products was filtered and washed by ethanol several times, and then dried under vacuum at 80 °C for 12 h to obtain the white product (yield: 98%).

2.3. Synthesis of cured epoxy resins

Formulas of cured epoxy resin samples were listed in Table 1. The preparation process of cured epoxy resins modified with MAPPO was follows: DGEBA and MAPPO were mixed together with a magnetic stirring at 100 °C for 30 min until a homogenous mixture was obtained. After that, DDM was poured into the above mixture, and was kept stirring for 2−3 min. Finally, the mixture was rapidly charged into mold, and cured at 100 °C for 2 h and 150 °C for 3 h. The EP was also prepared by the same procedure without MAPPO.

2.4. Measurements

Fourier transform infrared spectra (FT-IR) of samples were obtained using a Nicolet 6700 infrared spectrometer in the range of 4000–400 cm^{-1} at rt. The powder samples were mixed with KBr powders and pressed into tablets.

^{1}H and ^{31}P nuclear magnetic resonance (NMR) spectra of samples were recorded on a Bruker Ascend 400 spectrometer using DMSO as the solvent.

Thermogravimetry analysis (TG) test performed on thermogravimetric analyzer (TGA4000, USA). About 8 mg samples (MAPPO powder and cured EP resin pellets) were putted in alumina crucible and heated from 40 °C to 700 °C at a heating rate of 10 °C/min under nitrogen. In addition, the gases produced from thermal decomposition process from 40 to 700 °C at a heating rate of 10 °C/min were analyzed by FT-IR coupled with TG.

Differential scanning calorimeter (DSC) spectra were connected with a PE DSC 4000 at a heating rate of 10 °C/min from 40 °C to 200 °C under nitrogen flow of 50 mL/min.

LOI values were obtained using a HC-2C oxygen index instrument (Jiangning, China) according to ASTM D2863-97, with sheet sizes of 130 × 6.5 × 3.2 mm. UL-94 rating test was measured on a CZF-4 instrument (Jiangning, China) according to ASTM D3801, and the size of sheets was 130 × 13 × 3.2 mm. Cone calorimeter test was measured using a cone calorimeter (Fire Testing Technology, UK) according to ISO5660-1 at a heat radiant flux of 35 kW/m^2, and the size of each sample was 100 × 100 × 3.2 mm.

Table 1
LOI and UL-94 results of EP and EP/MAPPO samples.

Sample	DGEBA (%)	DDM (%)	MAPPO (%)	UL-94	LOI (%)
EP	80	20	0	NR	25.6 ± 0.5
EP/5MAPPO	76	19	5	NR	32.2 ± 0.5
EP/10MAPPO	72	18	10	V-1	33.3 ± 0.5
EP/15MAPPO	68	17	15	V-1	34.0 ± 0.5
EP/18MAPPO	65.6	16.4	18	V-0	33.0 ± 0.5

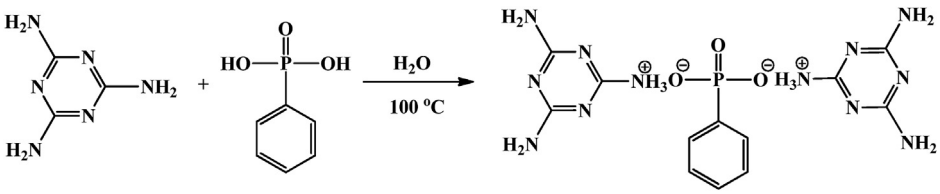

Scheme 1. Route for synthesis of MAPPO.

The micromorphology of chars after cone calorimeter test was observed using a JEOL JSM-5900LV scanning electron microscopy (SEM) instrument in a high vacuum at a voltage of 20 kV.

The LabRAM HR800 laser Raman spectrometer (SPEX Co.) was carried out to analyze the char structure with a 532 nm helium-neon laser line at room temperature.

3. Results and discussion

3.1. Characterization of MAPPO

The structure of MAPPO was firstly characterized by FT-IR, Fig. 1 showed the IR spectra of PPOA, MA and MAPPO. For PPOA, three characteristic peaks at 2732 cm^{-1}, 1438 cm^{-1} and 1149 cm^{-1} were observed, which belonged to P—OH, benzene ring and P═O groups, respectively. For MA, the peaks at 3468 cm^{-1}, 3418 cm^{-1}, 3331 cm^{-1} and 3123 cm^{-1} were attributed to different NH_2- bonds of MA [30]. The peak at 1650 cm^{-1} was assigned to C═N bond. For MAPPO, by comparison with MA, both the change of the position of C═N which moved from 1650 to 1676 cm^{-1} and the appearance of P═O bond, suggesting PPOA was successfully attached to the molecule of MA [31].

The structure of MAPPO was further confirmed by NMR test. In Fig. 2(a), compared with PPOA, the new peak appeared at 6.7 ppm, which was assigned to NH_2- groups of MA. Meanwhile, the ratio of integrated areas of a: b: c was 2: 3: 12, which was in accordance with the number ratio of corresponding hydrogen protons in MAPPO. Moreover, Fig. 2 (b) presented the ^{31}P NMR of PPOA and MAPPO. In Fig. 2(b), the position of P atom of PPOA at 12.79 ppm, while the position of P atom of MAPPO moved to 11.23 ppm since the electron cloud of both oxygen anion was dispersed by the ionic bond after salt formation. The results of IR and NMR implied that the target product MAPPO was successfully prepared. Table 2 showed the elemental contents of MAPPO. As seen in Table 2, the experimental value of C, H and N were approximately equal to calculated value. The above results confirmed that the target product (MAPPO) was successfully prepared.

Thermal decomposition behavior of MAPPO was also investigated by TG test, Fig. 3 showed the TGA and DTG curves of MAPPO. As seen, the onset decomposition temperature ($T_{5\%}$, defined as the temperature at which 5 wt% mass loss) of MAPPO was 264.5 °C, and presented mainly four stage decompositions with 16 wt% residual mass at 700 °C. The temperature at the maximum mass loss rate (T_{max}) of MAPPO was 287 °C, 360 °C, 515 and 620 °C, respectively. To further analyze the gaseous product released in heating process,

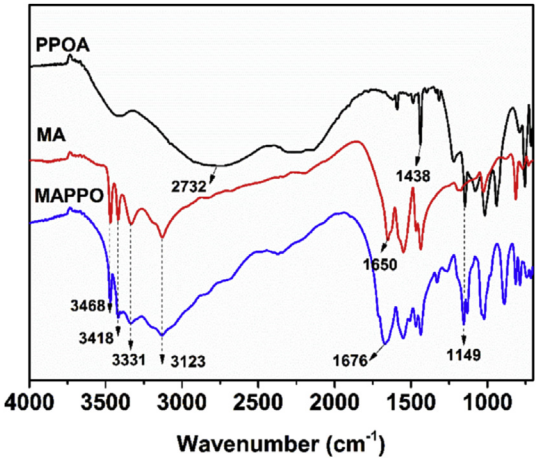

Fig. 1. IR spectra of PPOA, MA and MAPPO.

TG-IR test was carried out. As seen in Fig. 4, the main gaseous products at the temperature range from 250 °C to 450 °C were CO_2 and H_2O, which was mainly caused by the breaking of a part of C—N, the dehydrogenation of melamine and the dehydration phosphoric-containing acid [29]. As the temperature increased from 450 °C to 600 °C, MAPPO produced NH_3 (965, 932 cm^{-1}), —OH (3547 cm^{-1}), C═N (1558 cm^{-1}), C≡N (2245 cm^{-1}) [31,32], amines and aromatic compounds (3091 cm^{-1}), which was attributed to the ring-opening reactions of triazine and benzene rings [33].

3.2. Flame retardancy and combustion behavior

Flame retardancy of EP and flame-retardant EP was investigated by LOI and UL-94 tests. As seen in Table 1, EP was flammable with a LOI value of 25.6% and failed to UL-94 test. Adding 10 wt% MAPPO allowed EP/10MAPPO to pass UL-94 V-1 rating. Further increasing the content of MAPPO to 18 wt%, the EP/18MAPPO successfully reached V-0 rating. For LOI tests, after adding 5 wt% MAPPO, the LOI value of EP/5MAPPO achieved 32%. However, with the increasing addition of MAPPO, the LOI value of EP/MAPPO increased slightly, and EP/15MAPPO had a highest LOI value of 34%. It suggested that the phosphorus component of MAPPO was mainly worked in the condensed phase, and the fuel dilution effects of ammonia gas was inefficient at high oxygen concentration atmosphere [22,34].

Cone calorimeter test is an effective bench scale way to evaluate the combustion behavior of materials, which provides many important parameters including the time to ignition (TTI), peak of heat release rate (PHRR), time to PHRR (t_p), total heat release (THR), peak of smoke production rate (PSPR), total smoke production (TSP), total smoke release (TSR), average CO yield (av-COY), average rate of heat emission (ARHE), average effective heat of combustion (av-EHC) and char residues, etc. Fig. 5 presented the curves of HRR, THR, ARHE and TSP, and corresponding data were listed in Table 3.

As seen in Fig. 5 (a), EP had a high PHRR value of 1073 kW/m^2, while the HRR value of EP/18MAPPO decreased to 443 kW/m^2 with a reduction of 58.7%, which was caused by rapid char formation and fuel dilution of non-combustible gases produced by MAPPO in advance [29]. The pictures of char residues were shown in Fig. 6, epoxy resin almost burned out, while EP/18MAPPO showed a strongly expanded carbon residue with a residual mass of up to 31.6%, which served as a good barrier to insolute the transfer of heat and oxygen and proved the existence of condensed phase activity during combustion [35]. A large amount of decomposition products of EP were participated in charring instead of burning, resulting in the direct reduction of fuel and soot particles which were incomplete combustion. As seen in Table 3, it was clear that the peak of smoke production rate (PSPR) and total smoke production (TSP) of EP/18MAPPO were remarkable reduced compared with those of EP, which were reduced by 49% and 61.6% respectively. Because of the good inhibition founction of the combustion, the THR value of EP/18MAPPO decreased by 40% as well. However, the value of EHC, which related to the burning degree of volatile gases in gaseous phase during combustion, was slightly decreased by 8.5%, and the CO yield was no significant change with MAPPO addition. This result suggested that there was few fragments with free radical trapping formed in the gaseous phase, and the fuel-dilution by non-flammable gas such as NH_3, H_2O was the major flame-retardant mechanism in gaseous phase. In addition, to further evaluate the fire safety of epoxy resin, fire growth rate (FIGRA, defined as the maximum value of HRR/t and was always equal to PHRR/t_p) and maximum average rate of heat emission (MARHE, defined as the maximum value of THR (t)/t where t was the testing time) were also calculated. Compared with EP, the FIGRA and MARHE values of EP/18MAPPO were largely decreased, demonstrating adding MAPPO was able to slow down the combustion rate, and improve the flame

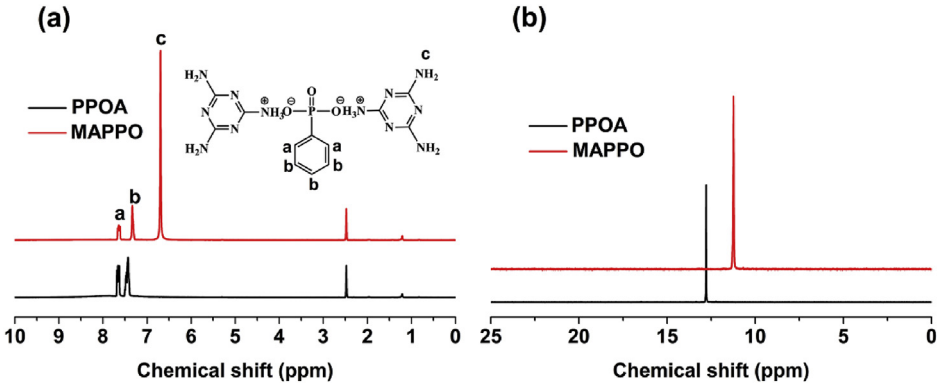

Fig. 2. ^{1}HNMR (a) and ^{31}PNMR (b) spectra of PPOA and MAPPO.

Table 2
Elemental contents of MAPPO.

Sample	Cal. (wt%)			Exp. (wt%)		
	C	H	N	C	H	N
MAPPO	35.12	4.67	40.96	34.62	4.53	41.42

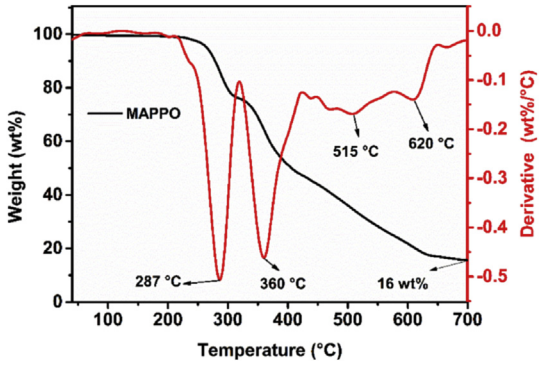

Fig. 3. TG and DTG curves of MAPPO under N_2.

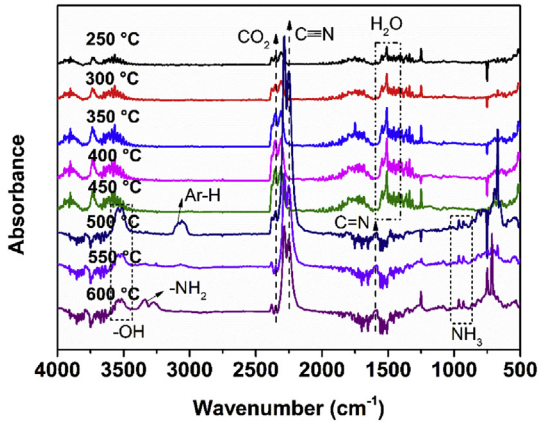

Fig. 4. TG-FTIR spectra of the pyrolysis products of MAPPO at different temperature.

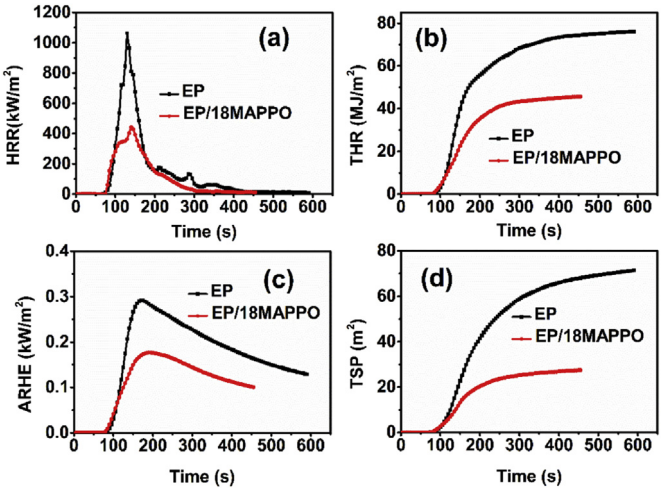

Fig. 5. The curves of HRR (a), THR (b), ARHE (c) and TSP (d) of EP and EP/18MAPPO after cone calorimeter test.

Table 3
Cone calorimeter data of EP and EP/18MAPPO.

Sample	EP	EP/18MAPPO
TTI (s)	60 ± 1	68 ± 2
t_P (s)	130 ± 3	140 ± 4
PHRR (kW/m^2)	1073 ± 55	443 ± 20
FIGRA ((kW/m^2·s)	8.3	3.2
THR (MJ/m^2)	76 ± 3	46 ± 2
MARHE (kW/m^2)	291.6	176.9
PSPR (m^2/s)	0.55 ± 0.02	0.28 ± 0.01
TSP (m^2)	71.4 ± 3	27.4 ± 1
TSR (m^2/m^2)	5241 ± 400	3015 ± 200
av-COY	0.095 ± 0.01	0.094 ± 0.01
av-EHC	21.1 ± 1	19.3 ± 1
Char residue (wt %)	10.2 ± 0.5	31.6 ± 1.5

retardancy of EP [36,37].

3.3. Thermal behavior analysis

Glass transition temperature (T_g) of EP and flame-retardant EP was investigated by DSC, and the corresponding data shown in Fig. 7. From Fig. 7, all samples showed a single T_g, and the EP poesses the highest T_g value of 159 °C. With the addition of MAPPO, the T_g value of EP/MAPPO samples was decreased gradually. This was mainly due to the large free volume and stereo-hindrance of

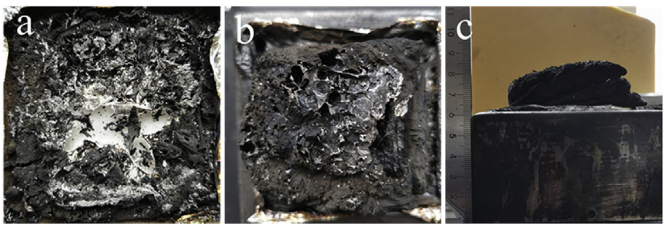

Fig. 6. Digital photos of char residues for EP (a), EP/18MAPPO (b,c) after cone calorimeter test.

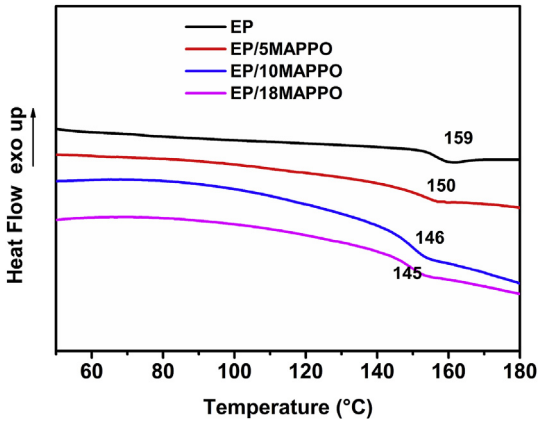

Fig. 7. DSC curves of EPand EP/MAPPO samples.

MAPPO, resulting in the decrease of the crosslinking degree of the EP/MAPPO system [38].

Fig. 8 showed the TG and DTG curves of MAPPO, and corresponding data were collected in Table 4. For EP, it began to decompose at 355.8 °C ($T_{5\%}$) and showed one-step decomposition with a maximum weight mass loss rate at 380.5 °C and a residual mass of 20.2 wt%. The thermal decomposition of EP at 380.5 °C (T_{max}) was contributed to the breakage of crosslinked molecular chain of EP itself [39]. For EP/MAPPO samples, the $T_{5\%}$ and T_{max} decreased gradually with the increase of the addition amount of MAPPO, which was caused by the early decomposition of MAPPO. However, the residual mass of EP/MAPPO samples at 700 °C was higher than that of EP, and the rate at T_{max} of all EP/MAPPO samples was reduced. The reason was that MAPPO decomposed in advance to produce some phosphoric-containing acid, acting as dehydrating agents to catalyze the degradation and carbonization of EP.

3.4. Flame-retardant mechanism

To investigate the condensed phase mechanism of EP/MAPPO system, char residues after cone calorimeter test were analyzed by SEM, IR and Raman. As seen in Fig. 9, the char layer of EP was rough and had many apparent crevices. Compared with EP, the char layer of EP/18MAPPO was relatively smooth and compact, suggesting that MAPPO was able to improve the quality of char residue during combustion.

The element composition of the char residues were investigated by EDX, and the relevant data were listed in Table 5. It was found that the composition of phosphorus in the char residue of EP/18MAPPO was higher than the theoretical value of phosphorus content added into the cured EP/18MAPPO (1.36 wt%), which indicated phosphorus derived from MAPPO mainly left in the char residue as well.

Raman spectroscopy was considered to be an effective method for measuring the order degree of carbon residues and corresponding data were shown in Fig. 10. Two peaks at 1358 cm^{-1} and 1560 cm^{-1} were observed in Fig. 10, which were assigned to D and G bonds, respectively. Generally, the D bond was owing to disordered graphite or glassy carbon, and the G bond belonged to vibration of sp^2-hybridized aromatic layers. Basically, R value equaled to the I_D/I_G (defined as intensities ratio of D bond to G bond) which was assessed the degree of graphitization, and the higher R value meant the lower the graphitization degree [40]. As seen, the R value of EP/18MAPPO (3.34) was lower than that of EP (4.03), implying the char layer of EP/18MAPPO with graphitization structure play a

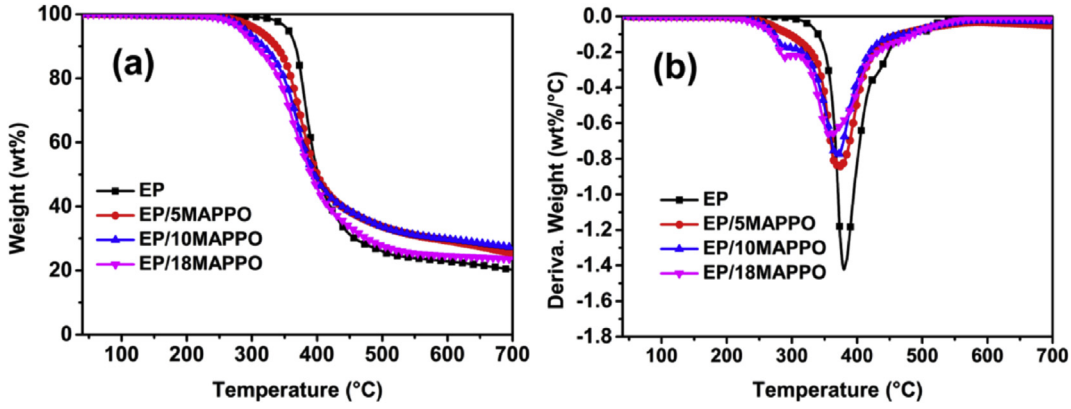

Fig. 8. TGA (a) and DTG (b) curves of EP and flame-retardant EP/MAPPO samples.

Table 4
TGA and DTG data of MAPPO, EP and EP/MAPPO samples.

Sample	$T_{5\%}$ (°C)	T_{max} (°C)	Rate at T_{max} (%/min)	Residue at 700 °C (wt%)
EP	355.8	380.5	1.4	20.2
EP/5MAPPO	309.5	372.7	0.84	25.2
EP/10MAPPO	290.1	369.2	0.78	27.1
EP/18MAPPO	285.1	359.2	0.66	23.6

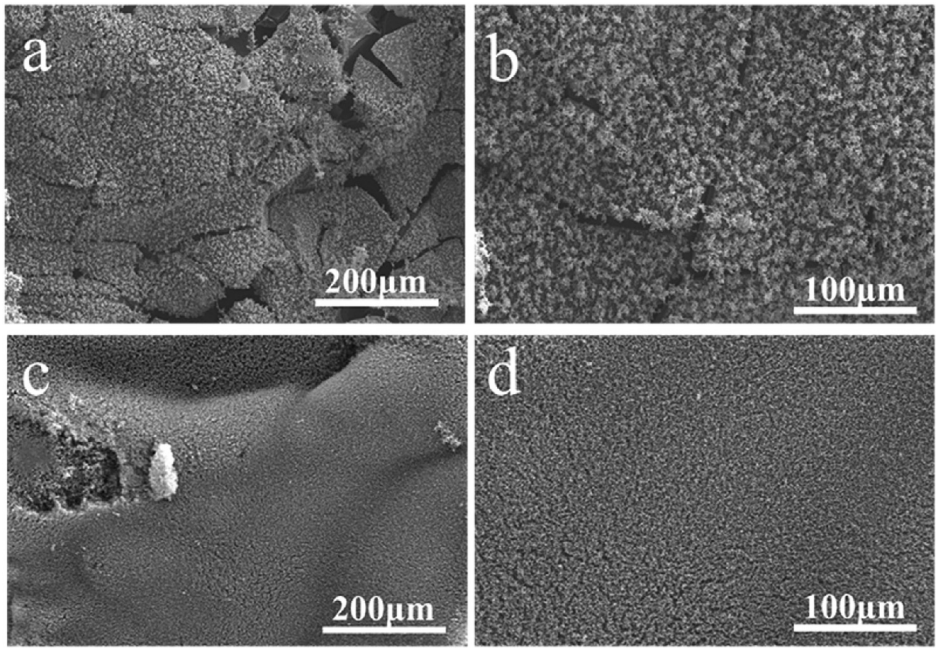

Fig. 9. SEM images of char residues for EP (a, b) and EP/18MAPPO (c, d).

better role in the insulation of heat and oxygen.

The concentration of char residues was further analyzed by IR. In Fig. 11, the absorption peaks at about 3000 cm^{-1} and 1609 cm^{-1} were assigned to CH_2- and C═C bonds, respectively. However, some differences were found in EP/18MAPPO. The peaks at 1231 cm^{-1} and 1176 cm^{-1} belong to P═O and P–O–C bonds, respectively, demonstrating some organophosphorus compounds exited in char residues after burning [41]. The above results proved that some compounds produced by MAPPO accelerated the cross-linking of EP degradation products to form some stable and compact char residues rich in organophosphorus compounds.

Based on the above analysis, the flame-retardant mechanism of EP/MAPPO system was concluded as follows. In the gaseous phase, MAPPO generated a large of nonflammable gases, such as NH_3, CO_2 and H_2O, which diluted oxygen and fuel gases produced by decomposition of epoxy resin as well as took away the heat during combustion. In the condensed phase, the poly-/pyro-/ultraphosphoric acids generated from degradation of MAPPO would react with epoxy resin through the dehydration and carbonization. Large amount of EP molecular fragments remained in the condensed phase to promote the formation of expanded char layer with P–O–C structure. This expanded char layer was able to serve as a good barrier to restrict the heat and oxygen transfer. Consequently, the enhancement in flame retardancy was attributed to the diluting effect of nonflammable gases and the barrier effect of expanded char residues with P–O–C structure at the same time.

4. Conclusions

In this paper, a novel phosphorus-nitrogen flame retardant named as MAPPO was synthesized successfully by the neutralization reaction and used to improve the flame retardancy of EP. As expect, by incorporation of 18 wt% MAPPO, epoxy resin not only passed the UL-94 V-0 rating and achieved a high LOI value of 33%, but also significantly suppressed the heat release and smoke

Table 5
Element composition of the char residues for EP/18MAPPO after combustion.

Sample	C (wt%)	O (wt%)	N (wt%)	P (wt%)
EP/18MAPPO	80.2	11.3	4.8	3.7

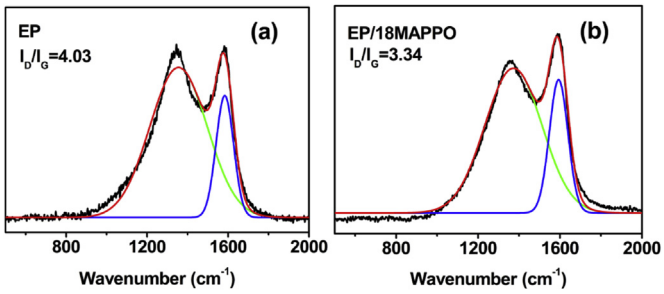

Fig. 10. Raman spectra of char residues for EP (a) and EP/18MAPPO (b).

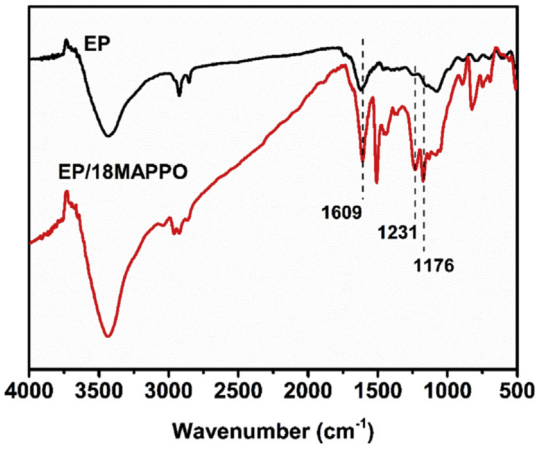

Fig. 11. IR spectra of char residues for EP and EP/18MAPPO.

production. By the analysis of TG-IR, SEM, IR and Raman, it gave a clear conclusion that the improvement in flame retardancy was contributed to both gaseous and condensed phase. In gaseous phase, some non-flammable gases such as NH_3, CO_2 and H_2O diluted the concentration of oxygen and fuel gases to slow down the combustion. In condensed phase, phosphorus-containing acids produced in high temperature would react with epoxy resin by dehydration and carbonization to form a stable and compact char layer, which was used as a good protective layer to interrupt the combustion.

Acknowledgments

This work was financially supported by the National Natural Science Foundation of China (Grant 51803195).

References

[1] B. Schartel, A.I. Balabanovich, U. Braun, U. Knoll, J. Artner, M. Ciesielski, et al., Pyrolysis of epoxy resins and fire behavior of epoxy resin composites flame retarded with 9, 10-dihydro-9-oxa-10-phosphaphenanthrene-10-oxide additives, J. Appl. Polym. Sci. 104 (2007) 2260–2269.
[2] Q.Q. Luo, Y.L. Sun, B. Yu, C.P. Li, J.L. Song, D.X. Tan, J.Q. Zhao, Synthesis of a novel reactive type flame retardant composed of phenophosphazine ring and maleimide for epoxy resin, Polym. Degrad. Stab. 165 (2019) 137–144.
[3] S. Yang, Y.F. Hu, Q.X. Zhang, Synthesis of a phosphorus-nitrogen containing flame retardant and its application in epoxy resin, High Perform. Polym. 31 (2019) 186–196.
[4] L. Yan, Z.S. Xu, X.H. Wang, N. Deng, Z.Y. Chu, Preparation of a novel monocomponent intumescent flame retardant for enhancing the flame retardancy and smoke suppression properties of epoxy resin, J. Therm. Anal. Calorim. 134 (2018) 1505–1519.
[5] S.L. Jin, L.J. Qian, Y. Qiu, Y.J. Chen, F. Xin, High-efficiency flame retardant behavior of bi-DOPO compound with hydroxyl group on epoxy resin, Polym. Degrad. Stab. 166 (2019) 344–352.
[6] P. Müller, M. Morys, A. Sut, C. Jäger, B. Illerhaus, B. Schartel, Melamine poly(zinc phosphate) as flame retardant in epoxy resin: decomposition pathways, molecular mechanisms and morphology of fire residues, Polym. Degrad. Stab. 130 (2016) 307–319.
[7] G. Grause, D. Karakita, J. Ishibashi, T. Kameda, T. Bhaskar, T. Yoshioka, TG-MS investigation of brominated products from the degradation of brominated flame retardants in high-impact polystyrene, Chemosphere 85 (2011) 368–373.
[8] M.M. Velencoso, A. Battig, J.C. Markwart, B. Schartel, F.R. Wurm, Molecular firefighting—how modern phosphorus chemistry can help solve the challenge of flame retardancy, Angew. Chem. Int. Ed. 57 (2018) 10450–10467.
[9] H.H. Liao, Y.S. Liu, J. Jiang, J. Li, Y. Liu, Synergism and antagonism of phosphorus-containing epoxy resin combined with different metal hydroxides, J. Fire Sci. 34 (2016) 3–12.
[10] M. Rakotomalala, S. Wagner, M. Döring, Recent developments in halogen free flame retardants for epoxy resins for electrical and electronic applications, Materials 3 (2010) 4300–4327.
[11] S. Bourbigot, S. Duquesne, Fire retardant polymers: recent developments and opportunities, J. Mater. Chem. 17 (2007) 2283–2300.
[12] Z.B. Shao, M.X. Zhang, Y. Li, Y. Han, L. Ren, C. Deng, A novel multi-functional polymeric curing agent: synthesis, characterization, and its epoxy resin with simultaneous excellent flame retardance and transparency, Chem. Eng. J. 345 (2018) 471–482.
[13] S. Levchik, A. Piotrowski, E. Weil, Q. Yao, New Developments in Flame Retardancy of Epoxy Resins, UBC Press, 2005, pp. 57–62.
[14] R.K. Jian, P. Wang, L. Xia, X.L. Zheng, Effect of a novel P/N/S-containing reactive flame retardant on curing behavior, thermal and flame-retardant properties of epoxy resin, J. Anal. Appl. Pyrolysis 127 (2017) 360–368.
[15] S.V. Levchik, E.D. Weil, A review of recent progress in phosphorus-based flame retardants, J. Fire Sci. 24 (2006) 345–364.
[16] Q.Q. Zhang, S. Yang, J. Wang, J.W. Cheng, Q.X. Zhang, G.P. Ding, Y.F. Hu, S.Q. Huo, A DOPO based reactive flame retardant constructed by multiple heteroaromatic groups and its application on epoxy resin: curing behavior, thermal degradation and flame retardancy, Polym. Degrad. Stab. 167 (2019) 10–20.
[17] M.J. Chen, Y.C. Lin, X.N. Wang, L. Zhong, Q.L. Li, Z.G. Liu, Influence of cuprous oxide on enhancing the flame retardancy and smoke suppression of epoxy resins containing microencapsulated ammonium polyphosphate, Ind. Eng. Chem. Res. 54 (2015) 12705–12713.
[18] W. Zhao, J.P. Liu, H. Peng, J.Y. Liao, X.J. Wang, Synthesis of a novel PEPA-substituted polyphosphoramide with high char residues and its performance as an intumescent flame retardant for epoxy resins, Polym. Degrad. Stab. 118 (2015) 120–129.
[19] X. Wang, Y. Hu, L. Song, W.Y. Xing, H.D. Lu, P. Lv, G.X. Jie, Effect of a triazine ring-containing charring agent on fire retardancy and thermal degradation of intumescent flame retardant epoxy resins, Polym. Adv. Technol. 22 (2011) 2480–2487.
[20] Y.J. Xu, J. Wang, Y. Tan, M. Qi, L. Chen, Y.Z. Wang, A novel and feasible approach for one-pack flame-retardant epoxy resin with long pot life and fast curing, Chem. Eng. J. 337 (2018) 30–39.
[21] B. Dittrich, K.A. Wartig, R. Mülhaupt, B. Schartel, Flame-retardancy properties of intumescent ammonium poly(phosphate) and mineral filler magnesium hydroxide in combination with graphene, Polymers 6 (2014) 2875–2895.
[22] R.K. Jian, Y.F. Ai, L. Xia, L.J. Zhao, H.B. Zhao, Single component phosphamide-based intumescent flame retardant with potential reactivity towards low flammability and smoke epoxy resins, J. Hazard Mater. 371 (2019) 529–539.
[23] L. Yan, Z.S. Xu, X.H. Wang, Synergistic effects of organically modified montmorillonite on the flame-retardant and smoke suppression properties of transparent intumescent fire-retardant coatings, Prog. Org. Coat. 122 (2018) 107–118.
[24] G. Camino, L. Costa, G. Martinasso, Intumescent fire-retardant systems, Polym. Degrad. Stab. 23 (1989) 359–376.
[25] Y. Tan, Z.B. Shao, X.F. Chen, J.W. Long, L. Chen, Y.Z. Wang, Novel multifunctional organic–inorganic hybrid curing agent with high flame-retardant efficiency for epoxy resin, ACS Appl. Mater. Interfaces 7 (2015) 17919–17928.
[26] L. Zheng, K.X. Zhang, X. Wang, M.J. Chen, F. Xin, Z.G. Liu, Synergistic effects and flame-retardant mechanism of aluminum diethyl phosphinate in combination with melamine polyphosphate and aluminum oxide in epoxy resin, J. Therm. Anal. Calorim. 134 (2018) 1637–1646.
[27] Y. Tan, Z.B. Shao, L.X. Yu, J.W. Long, M. Qi, L. Chen, Y.Z. Wang, Piperazine modified ammonium polyphosphate as monocomponent flame-retardant hardener for epoxy resin: flame retardance, curing behavior and mechanical property, Polym. Chem. 7 (2016) 3003–3012.
[28] M.J. Chen, Y.C. Lin, X.N. Wang, L. Zhong, Q.L. Li, Z.G. Liu, Influence of cuprous oxide on enhancing the flame retardancy and smoke suppression of epoxy resins containing microencapsulated ammonium polyphosphate, Ind. Eng. Chem. Res. 54 (2015) 12705–12713.
[29] Z.M. Zhu, L.X. Wang, L.P. Dong, Influence of a novel P/N-containing oligomer on flame retardancy and thermal degradation of intumescent flame-retardant epoxy resin, Polym. Degrad. Stab. 162 (2019) 129–137.
[30] S. Shang, B.H. Yuan, Y.R. Sun, G.Q. Chen, C.Y. Huang, B. Yu, S. He, H.M. Dai, X.F. Chen, Facile preparation of layered melamine-phytate flame retardant via supramolecular self-assembly technology, J. Colloid Interface Sci. 553 (2019) 364–371.
[31] M.J. Chen, Z.B. Shao, X.L. Wang, L. Chen, Y.Z. Wang, Halogen-free flame-retardant flexible polyurethane foam with a novel nitrogen-phosphorus flame retardant, Ind. Eng. Chem. Res. 51 (2012) 9769–9776.
[32] W.H. Rao, Z.Y. Hu, H.X. Xu, Y.J. Xu, M. Qi, W. Liao, S.M. Xu, Y.Z. Wang, Flame-retardant flexible polyurethane foams with highly efficient melamine salt, Ind. Eng. Chem. Res. 56 (2017) 7112–7119.
[33] Z.M. Bai, X. Wang, G. Tang, L. Song, Y. Hu, R.K.K. Yuen, Structure-property relationships of synthetic organophosphorus flame retardant oligomers by thermal analysis, Thermochim. Acta 565 (2013) 17–26.
[34] S. Brehme, T. Köppl, B. Schartel, V. Altstädt, Competition in aluminium phosphinate-based halogen-free flame retardancy of poly(butylene terephthalate) and its glass-fibre composites, E-Polymers 14 (2014) 193–208.
[35] B. Schartel, T.R. Hull, Development of fire-retarded materials—interpretation of cone calorimeter data, Fire Mater. 31 (2007) 327–354.
[36] Z.M. Zhu, Y.J. Xu, W. Liao, S.M. Xu, Y.Z. Wang, Highly flame retardant expanded polystyrene foams from phosphorus-nitrogen-silicon synergistic adhesives, Ind. Eng. Chem. Res. 56 (2017) 4649–4658.
[37] Y.X. Wei, C. Deng, Z.Y. Zhao, Y.Z. Wang, A novel organic-inorganic hybrid SiO2@DPP for the fire retardance of polycarbonate, Polym. Degrad. Stab. 154 (2018) 177–185.
[38] Y. Zhang, B. Yu, B.B. Wang, K.M. Liew, L. Song, C.M. Wang, Y. Hu, Highly effective P-P synergy of a novel DOPO-based flame retardant for epoxy resin, Ind. Eng. Chem. Res. 56 (2017) 1245–1255.
[39] W.J. Liang, B. Zhao, P.H. Zhao, C.Y. Zhang, Y.Q. Liu, Bisphenol-S bridged penta(anilino)cyclotriphosphazene and its application in epoxy resins: synthesis, thermal degradation, and flame retardancy, Polym. Degrad. Stab. 135 (2017) 140–151.
[40] Z. Li, A.J. Gonzalez, V.B. Heeralal, D.Y. Wang, Covalent assembly of MCM-41 nanospheres on graphene oxide for improving fire retardancy and mechanical property of epoxy resin, Compos. B Eng. 138 (2018) 101–112.
[41] G. Yang, W.H. Wu, Y.H. Wang, Y.H. Jiao, L.Y. Lu, H.Q. Qu, X.Y. Qin, Synthesis of a novel phosphazene-based flame retardant with active amine groups and its application in reducing the fire hazard of epoxy resin, J. Hazard Mater. 366 (2018) 78–87.